Local measurement of the entanglement between two quantum-dot qubits

Jin Liu,[1] Zhao-Tan Jiang,[1,2,*] and Bin Shao[1]
[1]*Department of Physics, Beijing Institute of Technology, Beijing 100081, People's Republic of China*
[2]*The Abdus Salam International Centre for Theoretical Physics, Strada Costiera 11, 34014 Trieste, Italy*
(Received 9 October 2008; revised manuscript received 17 February 2009; published 30 March 2009)

Using the modified rate equation the local measurement of the entanglement between two quantum-dot qubits, with two isolated quantum-point-contact detectors, is investigated. It is shown that the measurement process will induce the decaying of the two-qubit entanglement, as well as the electron-occupation probabilities. Furthermore, we find an effective scheme to measure the two-qubit entanglement based on the local measurement. It is demonstrated that the entanglement between the two qubits coupled by the strong Coulomb interaction can be fully extracted according to the time-dependent variation rate of the detector current.

DOI: 10.1103/PhysRevB.79.115323 PACS number(s): 73.21.La, 03.65.Ud, 03.67.−a

I. INTRODUCTION

Quantum measurement (QM) of the entanglement, an important parameter for quantum information processing, is considered to be one of the most crucial steps in the field of quantum information.[1] The methods of measuring quantum entanglement are still being extensively investigated both theoretically and experimentally. In general, based on the working principles of detectors QM can be classified into three kinds: the local measurement, the correlation one, and the joint one. Intuitively, one would believe that the local measurement cannot provide as much information as the other two kinds of measurements because in the local measurement scheme the detector only acts on part of the entire system. Usually, it is believed that the whole entanglement information can be extracted by the method of the joint measurement. Therefore, much effort has been made to investigate the joint measurement scheme.[2–17] Tanamoto and Hu[13] showed that the quantum-point-contact (QPC) current can be used for reading out the results of quantum computation and providing the information about the two-qubit entanglement. To our knowledge, however, little attention has been paid to the local measurement scheme.

In this paper, we design a local measurement scheme based on the quantum-dot (QD) system, as shown in Fig. 1. Each qubit is composed of two QDs (0 and 1) with one extra electron residing in it. When the electron occupies QD 0 or 1, the corresponding qubit state is $|0\rangle$ or $|1\rangle$. The qubit-i ($i=1,2$) states can be detected by measuring the current flowing through the nearby QPC i (detector). Note that this setup can be easily fabricated in two-dimensional electron gas based on the current experimental nanotechnology.[18] According to the method proposed by Gurvitz and Prager[19] we first derive the modified rate equation of the two-qubit system and then investigate the QM of the entanglement between the two qubits numerically. It is found that the electron-occupation probabilities and the entanglement evolve as a function of time. The mechanism of QM and the influences on the qubits induced by QM are further studied in detail by analyzing the currents flowing through the QPC detectors. The measurement process is found to induce the decays of both the electron-occupation probabilities and the entanglement. Notably, we demonstrate that the evolution of the entanglement can be *fully* extracted in some case from the time-dependent variation rate of the measured QPC currents. This indicates that in certain cases, the entanglement measurement can be accomplished by using the simple local measurement scheme alone, rendering the joint measurement unnecessary.

The rest of this paper is organized as follows. In Sec. II, we give the Hamiltonian of the two-qubit system and the modified rate equations. An analytical analysis is performed in Sec. III on the time-dependent evolution of the two qubits in the absence of detectors. Then in Sec. IV the numerical results and discussions about the two qubits coupled by the different coupling strengths are presented. Finally, a conclusion is outlined in Sec. V.

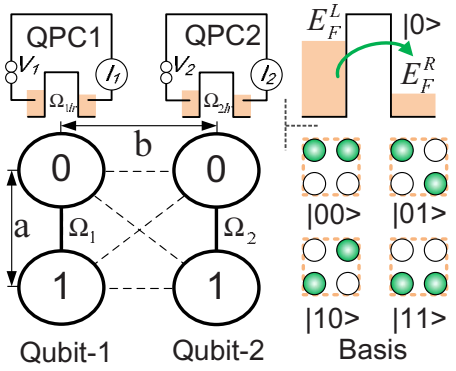

FIG. 1. (Color online) Schematic illustration of the quantum measurement of the entanglement between two quantum-dot qubits by two QPC detectors placed above. Each qubit is composed of two QDs labeled by 0 and 1. The interdot coupling between two QDs in each qubit is shown by the solid line, and the dashed lines denote the interdot Coulomb interactions. The quantum entanglement between qubit 1 and qubit 2 can be measured by the currents I_1 and I_2 flowing through the two detectors QPC1 and QPC2 with the biased voltages V_1 and V_2. The right upper picture shows the Fermi levels E_F^L and E_F^R of the detector in the initial vacuum state, and the arrow denotes the electron tunneling from the left lead to the right one. Moreover, shown in the right lower part are the four possible bases $|00\rangle$, $|01\rangle$, $|10\rangle$, and $|11\rangle$ of the two qubits where the filled circle denotes that there is one electron localized in it.

II. FORMULATION

The QD two-qubit system, schematically shown in Fig. 1, including two QPC detectors can be expressed by the Hamiltonian $H=H_S+H_{1D}+H_{2D}+H_I$, in which the two-qubit Hamiltonian is

$$H_S=\sum_{i,j}(E_{ij}c_{ij}^{\dagger}c_{ij}+U_{1i,2j}n_{1i}n_{2j})+\sum_i \Omega_i(c_{i0}^{\dagger}c_{i1}+\text{h.c.}). \tag{1}$$

Here E_{ij} denotes the ground-state energy of the jth QD in the ith qubit. $c_{ij}^{\dagger}$ (c_{ij}) is the creation (annihilation) operator of the electron on the energy level E_{ij}, and $n_{ij}\equiv c_{ij}^{\dagger}c_{ij}$ is the corresponding particle number operator. Ω_i represents the interdot coupling in the ith qubit, and $U_{1i,2j}$ denotes the Coulomb repulsion interaction between the two electrons in the two qubits. The Hamiltonian of the detector placed above qubit i is

$$H_{iD}=\sum_l E_{il}c_{il}^{\dagger}c_{il}+\sum_r E_{ir}c_{ir}^{\dagger}c_{ir}+\sum_{l,r}\Omega_{ilr}(c_{il}^{\dagger}c_{ir}+\text{h.c.}), \tag{2}$$

while the interaction between the two qubits and the two detectors can be modeled by

$$H_I=\sum_{lr}(\delta\Omega_{1lr}n_{10}c_{1l}^{\dagger}c_{1r}+\delta\Omega_{2lr}n_{20}c_{2l}^{\dagger}c_{2r}+\text{h.c.}). \tag{3}$$

Here $c_{il}^{(\dagger)}$ and $c_{ir}^{(\dagger)}$ represent the creation (annihilation) operators of the left-lead energy E_{il} and the right-lead energy E_{ir} in the ith detector, respectively. Ω_{ilr} is the coupling between the energy levels E_{il} and E_{ir}. $\delta\Omega_{ilr}$ denotes the coupling variation in the ith detector when the qubit electron enters QD-0 from QD-1. The wave function describing the entire system can be expressed as[19]

$$|\Psi(t)\rangle=\sum_{ij}\Bigg[b_{ij}(t)c_{1i}^{\dagger}c_{2j}^{\dagger}+\sum_{lr}b_{ijlr}(t)c_{1i}^{\dagger}c_{2j}^{\dagger}c_{1r}^{\dagger}c_{1l}+\sum_{pq}b_{ijpq}(t)c_{1i}^{\dagger}c_{2j}^{\dagger}c_{2q}^{\dagger}c_{2p}+\sum_{lrpq}b_{ijlrpq}(t)c_{1i}^{\dagger}c_{2j}^{\dagger}c_{1r}^{\dagger}c_{2q}^{\dagger}c_{1l}c_{2p}+\cdots\Bigg]|0\rangle. \tag{4}$$

Here, $b_{\ldots}(t)$ are the amplitudes of the probabilities finding the system in the states defined by the corresponding creation and annihilation operators. The so-called initial vacuum state $|0\rangle$ may be described in the following way: (i) the energy levels of the left and the right leads are filled up to their Fermi energy levels with $E_F^L \gg E_F^R$ as shown in Fig. 1, and (ii) four QDs in two qubits are kept empty. Throughout this research we consider the transport properties at *zero* temperature. The quantum evolution of the whole system is described by the time-dependent Schrödinger equation $i|\dot{\Psi}\rangle=H|\Psi\rangle$ and the corresponding density matrix is given by $\sigma(t)=|\Psi(t)\rangle\langle\Psi(t)|$. In the four-dimensional Fock space composed of (a) $|00\rangle$, (b) $|01\rangle$, (c) $|10\rangle$, and (d) $|11\rangle$ (see Fig. 1), where, for example, $|01\rangle$ denotes the qubit-1 electron occupies QD-0 and that of qubit-2 stays at QD-1, we can derive the differential equations of the reduced density matrix elements according to the procedure proposed by Gurvitz and Prager.[19] The diagonal matrix elements are expressed as

$$\dot{\sigma}_{aa}=i\Omega_1(\sigma_{ac}-\sigma_{ca})+i\Omega_2(\sigma_{ab}-\sigma_{ba}), \tag{5a}$$

$$\dot{\sigma}_{bb}=i\Omega_1(\sigma_{bd}-\sigma_{db})+i\Omega_2(\sigma_{ba}-\sigma_{ab}), \tag{5b}$$

$$\dot{\sigma}_{cc}=i\Omega_1(\sigma_{ca}-\sigma_{ac})+i\Omega_2(\sigma_{cd}-\sigma_{dc}), \tag{5c}$$

$$\dot{\sigma}_{dd}=i\Omega_1(\sigma_{db}-\sigma_{bd})+i\Omega_2(\sigma_{dc}-\sigma_{cd}), \tag{5d}$$

and the nondiagonal ones are[20]

$$\dot{\sigma}_{ab}=i(E_{ba}+U_{ba})\sigma_{ab}+i\Omega_1(\sigma_{ad}-\sigma_{cb})+i\Omega_2(\sigma_{aa}-\sigma_{bb})-\Gamma_{2d}\sigma_{ab}/2, \tag{6a}$$

$$\dot{\sigma}_{ac}=i(E_{ca}+U_{ca})\sigma_{ac}+i\Omega_1(\sigma_{aa}-\sigma_{cc})+i\Omega_2(\sigma_{ad}-\sigma_{bc})-\Gamma_{1d}\sigma_{ac}/2, \tag{6b}$$

$$\dot{\sigma}_{ad}=i(E_{da}+U_{da})\sigma_{ad}+i\Omega_1(\sigma_{ab}-\sigma_{cd})+i\Omega_2(\sigma_{ac}-\sigma_{bd})-(\Gamma_{1d}+\Gamma_{2d})\sigma_{ad}/2, \tag{6c}$$

$$\dot{\sigma}_{bc}=i(E_{cb}+U_{cb})\sigma_{bc}+i\Omega_1(\sigma_{ba}-\sigma_{dc})+i\Omega_2(\sigma_{bd}-\sigma_{ac})-(\Gamma_{1d}+\Gamma_{2d})\sigma_{bc}/2, \tag{6d}$$

$$\dot{\sigma}_{bd}=i(E_{db}+U_{db})\sigma_{bd}+i\Omega_1(\sigma_{bb}-\sigma_{dd})+i\Omega_2(\sigma_{bc}-\sigma_{ad})-\Gamma_{1d}\sigma_{bd}/2, \tag{6e}$$

$$\dot{\sigma}_{cd}=i(E_{dc}+U_{dc})\sigma_{cd}+i\Omega_1(\sigma_{cb}-\sigma_{aa})+i\Omega_2(\sigma_{cc}-\sigma_{dd})-\Gamma_{2d}\sigma_{cd}/2. \tag{6f}$$

For convenience we have defined the dephasing rate $\Gamma_{id}=(\sqrt{D_i}-\sqrt{D_i'})^2$, where $D_i=2\pi\rho_L\rho_R|\Omega_{ilr}|^2V_i$ or $D_i'=2\pi\rho_L\rho_R|\Omega_{ilr}'|^2V_i$ is the transition rate of an electron hopping from the left lead to the right one when the electron stays in QD-0 or QD-1 of qubit i. Here, ρ_L and ρ_R are the densities of states for the left and right leads, respectively, and V_i denotes the voltage bias between the left and right leads of QPC-i. Furthermore, according to the general current formula[19] $I_i(t)=dQ_{iR}(t)/dt=\Sigma_n n(\dot{\sigma}_{aa}^n+\dot{\sigma}_{bb}^n+\dot{\sigma}_{cc}^n+\dot{\sigma}_{dd}^n)$, with $Q_{iR}(t)$ being the total charge in the right lead and $\sigma_{\alpha\alpha}^n$ being the electron number resolved density matrix element, we can obtain the current flowing through the two detectors[21]

$$I_1=D_1'(\sigma_{aa}+\sigma_{bb})+D_1(\sigma_{cc}+\sigma_{dd}), \tag{7a}$$

$$I_2=D_2'(\sigma_{aa}+\sigma_{cc})+D_2(\sigma_{bb}+\sigma_{dd}). \tag{7b}$$

On the other hand, it has been demonstrated that nonpositivity of the partial transposition is a necessary and sufficient condition for describing the entanglement of a mixed state.[22] For a two-qubit system described by the density operator σ, the negativity criterion for the entanglement of the two qubits is given by the quantity $E=-2\Sigma_i u_i^-$ where the sum is taken over the negative eigenvalues u_i^- of the partial transposition of the density matrix σ. The value of $E=1$ corresponds to the maximum entanglement between the two qubits while $E=0$ indicates that the two qubits are separable.[22,23]

III. DYNAMICS OF COUPLED QUBITS

First we discuss the time-dependent properties of the two coupled qubits in the absence of detectors. For the isolated two coupled qubits, the corresponding Hamiltonian can be represented by H_S in Eq. (1). Using the basis vectors including $|a\rangle$, $|b\rangle$, $|c\rangle$, and $|d\rangle$, we can expand the wave function of the two-qubit system as $|\Psi(t)\rangle = f_a|a\rangle + f_b|b\rangle + f_c|c\rangle + f_d|d\rangle$. By substituting H_S and $|\Psi(t)\rangle$ into $i|\dot{\Psi}(t)\rangle = H_S|\Psi(t)\rangle$, we can easily obtain the coupled linear equations

$$i\dot{f}_a = (\varepsilon_a + U_a)f_a + \Omega_1 f_c + \Omega_2 f_b, \tag{8a}$$

$$i\dot{f}_b = (\varepsilon_b + U_b)f_b + \Omega_1 f_d + \Omega_2 f_a, \tag{8b}$$

$$i\dot{f}_c = (\varepsilon_c + U_c)f_c + \Omega_1 f_a + \Omega_2 f_d, \tag{8c}$$

$$i\dot{f}_d = (\varepsilon_d + U_d)f_d + \Omega_1 f_b + \Omega_2 f_c. \tag{8d}$$

Here we introduce $U_a = U_{00,10}$, $U_b = U_{00,11}$, $U_c = U_{01,10}$, and $U_d = U_{01,11}$ for convenience. In the limit of $U_{a,b,c,d} = 0$, we can obtain the time-dependent evolution formulation

$$\begin{pmatrix} f_a(t) \\ f_b(t) \\ f_c(t) \\ f_d(t) \end{pmatrix} = \frac{1}{2}\begin{pmatrix} r_2 & r_4 & r_3 & r_1 \\ r_4 & r_2 & r_1 & r_3 \\ r_3 & r_1 & r_2 & r_4 \\ r_1 & r_3 & r_4 & r_2 \end{pmatrix}\begin{pmatrix} f_a(0) \\ f_b(0) \\ f_c(0) \\ f_d(0) \end{pmatrix}, \tag{9}$$

where we define $r_1 = \cos(|\Omega_+|t) - \cos(|\Omega_-|t)$, $r_2 = \cos(|\Omega_+|t) + \cos(|\Omega_-|t)$, $r_3 = -i\sin(|\Omega_+|t) - i\sin(|\Omega_-|t)$, and $r_4 = -i\sin(|\Omega_+|t) + i\sin(|\Omega_-|t)$ with $\Omega_\pm \equiv \Omega_1 \pm \Omega_2$ and the initial values $f_{a,b,c,d}(0)$.

Then we consider the time-dependent evolution in the other limit of $U_{a,b,c,d} \to \infty$. We can obtain the relation

$$\begin{pmatrix} f_b(t) \\ f_c(t) \end{pmatrix} = \begin{pmatrix} \cos\omega t & i\sin\omega t \\ i\sin\omega t & \cos\omega t \end{pmatrix}\begin{pmatrix} f_b(0) \\ f_c(0) \end{pmatrix}, \tag{10}$$

in the initial conditions $f_a(0) = f_d(0) = 0$, and

$$\begin{pmatrix} f_a(t) \\ f_d(t) \end{pmatrix} = \begin{pmatrix} \cos\omega t & -i\sin\omega t \\ -i\sin\omega t & \cos\omega t \end{pmatrix}\begin{pmatrix} f_a(0) \\ f_d(0) \end{pmatrix}, \tag{11}$$

in the case of $f_a(0) = f_d(0) = 0$. Here ω is related to $\Omega_{1,2}$ and ΔU as $\omega = 2\Omega_1\Omega_2/\Delta U$ in the structure designed in Fig. 1. For simplicity, we have assumed that the four QDs are localized at the four vertices of a rectangle with length a and width b. Consider for example the evolution of the two qubits from a pure state $|b\rangle$ ($f_b = 1$ and $f_{a,c,d} = 0$) with equal interdot couplings $\Omega_1 = \Omega_2 = 1$. From Eq. (9) we can find that the probabilities $|f_{b,c}|^2$ in the basis vectors $|b,c\rangle$ will evolve in the period of π, while the oscillation periods of the probabilities $|f_{a,d}|^2$ are $\pi/2$. These oscillations with the period of π or $\pi/2$ are just a trivial effect induced by the partition of the usual Rabi oscillation of each qubit in the basis vectors $|a,b,c,d\rangle$. In the other limit case where the interdot Coulomb interaction is strong enough, the probabilities $|f_a|^2 = |f_d|^2 \approx 0$ and the probabilities $|f_b|^2 = \cos^2\omega t$ and $|f_c|^2 = \sin^2\omega t$, indicating the oscillation period is $\pi\Delta U/(2\Omega_1\Omega_2)$. It can be interpolated that the amplitudes of $|f_a(t)|^2$ and $|f_d(t)|^2$ will decrease to zero with increasing ΔU and the oscillation periods of $|f_b(t)|^2$ and $|f_c(t)|^2$ will become $\pi\Delta U/(2\Omega_1\Omega_2)$. This clearly demonstrates that the interdot Coulomb interactions will have an effect on the oscillation amplitudes and the periods. For a general ΔU, it is difficult to derive analytical results, and therefore a numerical study will be carried out in Sec. IV.

IV. NUMERICAL RESULTS

In this section we numerically study the dynamics of the two-qubit system based on the modified rate equations and explore how to extract the entanglement from the currents flowing through the QPC detector placed nearby. In view of the initialization of the qubit states and the Coulomb interaction between the two electrons in two qubits, here we assume that the initial state is chosen to be $\sigma_{bb}(0) = 1$ and all the other density matrix elements are kept to be zero at the time of $t = 0$. This means that the two-qubit system will evolve from a pure state to a mixed one. The Coulomb interactions denoted by the dashed lines between the two nearest QDs are chosen to be $U_{10,20} = U_{11,21} = \sqrt{2}U_{10,21} = \sqrt{2}U_{11,20} \equiv U$, and the interdot couplings $\Omega_1 = \Omega_2 = 1.0$ are used as the energy unit. In our calculation, we choose $D_1 = D_2 \equiv D$ and $D_1' = D_2' \equiv D' = 0.9D$ for clarity and the system temperature T is kept at 0 K.

A. Qubit dynamics without detector

In order to understand how to measure the two-qubit entanglement as well as the measurement-induced influences on the qubit information, it is instructive to examine in advance the dynamics of the two-qubit system in the absence of detectors ($D_{1,2} = 0$). First of all, the time-dependent evolutions of the electron-occupation probabilities σ_{bb} and σ_{cc} for the different interdot Coulomb interactions U are plotted in Fig. 2. In the case of $U = 0$, according to the relation in Eq. (9) the probabilities $\sigma_{bb}(t) = [\cos(2t) + 1]^2/4$ and $\sigma_{cc}(t) = [\cos(2t) - 1]^2/4$ exhibit the oscillations with a period of π. This oscillation, the well-known Rabi oscillation, is attributed to the interdot coupling, which induces the qubit electron to tunnel back and forth between QD0 and QD1. When the Coulomb interaction U becomes nonzero, obvious changes appear in the oscillations of σ_{bb} and σ_{cc}. For the moderately strong Coulomb interaction (e.g., $U = 5$ and 10) the oscillations exhibit complex patterns, which manifest the correlation effect induced by the interdot Coulomb interactions. With the further increase in U, the simple pattern of the periodical oscillations is restored for both σ_{bb} and σ_{cc}. This can be easily understood from a physical point of view. The interdot Coulomb interactions are inclined to force the two-qubit electrons to occupy the diagonal QDs separated by a larger interdot distance. To see the oscillations clearly, the Fourier transforms of the curves of σ_{bb} for different U are performed in Fig. 2(c). It is evident that the oscillation for $U = 0$ includes two main components with frequencies $f = 1$ and 2, just as indicated by relation (9). When U becomes nonzero, the oscillation pattern changes abruptly and three main components with different frequencies are observed. As U increases further, the amplitudes of the two higher-f oscil-

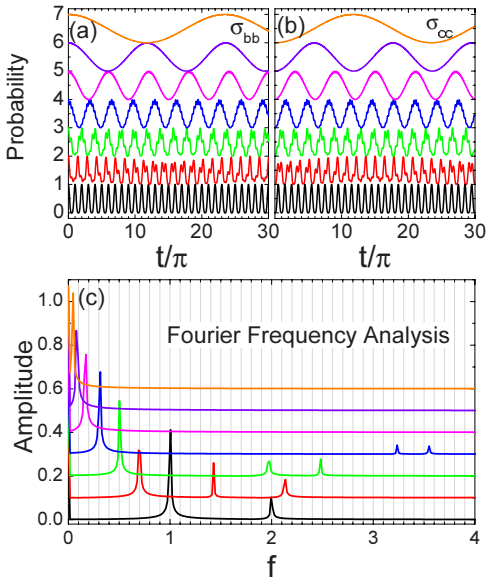

FIG. 2. (Color online) Time-dependent electron-occupation probabilities (a) σ_{bb} and (b) σ_{cc} with $D=0$. From bottom to top, the curves correspond to $U=0$, 5, 10, 20, 40, 80, and 160, respectively, which are shifted upward by 0, 1, 2, 3, 4, 5, and 6 for clarity. The corresponding Fourier transforms of $\sigma_{bb}(t)$ are shown in (c), and the curves are shifted from bottom to up by 0, 0.1, 0.2, 0.3, 0.4, 0.5, and 0.6, respectively.

lations become smaller and the corresponding frequencies become much higher, while the frequency of the lowest-f oscillation decreases continuously. In the large U limit, the two higher-f components diminish and only the lowest f survives. Obviously, the decrease in the frequency of the lowest-f oscillation indicates the increase in the oscillation period when U becomes strong. It should be emphasized that, in sharp contrast to the periodical oscillation of $U=0$, this kind of oscillation is closely dependent on the interdot Coulomb interaction U.

Furthermore, the oscillations of σ_{aa} or σ_{dd} corresponding to the case of Fig. 2 are shown in Fig. 3. For $U=0$, the probability $\sigma_{aa} \propto \sin^2(2t)$ or $\sigma_{dd} \propto \sin^2(2t)$ exhibits the oscillations with a period of $\pi/2$, which is due to the interdot coupling. When the interdot Coulomb interaction becomes nonzero, it is clear that σ_{aa} and σ_{dd} still oscillate periodically even in the case of moderately strong U. However, the period

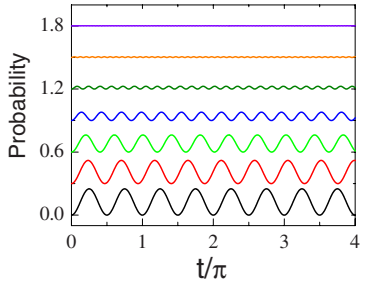

FIG. 3. (Color online) Time-dependent electron-occupation probability σ_{aa} or σ_{dd} with $D=0$. From bottom to top, the curves correspond to $U=0$, 5, 10, 20, 40, 80, and 160, which are shifted upward by 0, 0.3, 0.6, 0.9, 1.2, 1.5, and 1.8, respectively.

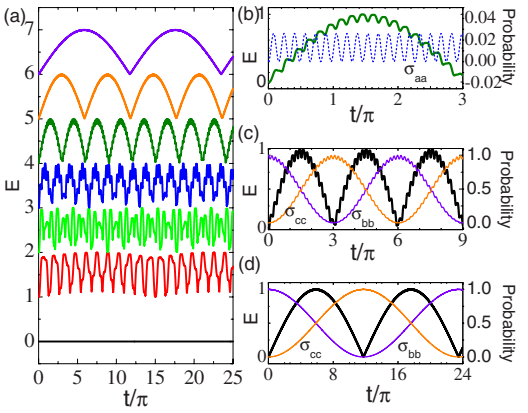

FIG. 4. (Color online) (a) Time-dependent entanglement E for the different interdot Coulomb interactions U. The parameters are the same as those in Fig. 2. (b) The entanglement and the corresponding probability σ_{aa} in the case of $U=40$. The entanglement and the corresponding probabilities σ_{bb} and σ_{cc} in the cases of (c) $U=40$ and (d) $U=160$.

of the oscillation is found to become smaller as U increases. Meanwhile, the oscillation amplitude also becomes much smaller. When U becomes sufficiently strong, as it should be, the amplitudes of σ_{aa} and σ_{dd} are inclined to approach zero, indicating that the two electrons in the two qubits cannot simultaneously occupy the state $|00\rangle$ or $|11\rangle$ anymore. This indicates that the interdot Coulomb interactions prevent the two electrons from occupying the nearest QDs. It should be emphasized that the interdot Coulomb interaction U does not induce complex oscillation patterns in the $\sigma_{aa}(t)$ and $\sigma_{dd}(t)$ curves, which are different from the case of σ_{bb} and σ_{cc}.

Next, we turn to investigate the entanglement between the two qubits based on the nonpositive partial transpose (NPT). Figure 4(a) shows the time-dependent evolutions of the quantum entanglement for the different interdot Coulomb interactions U. When the Coulomb interaction $U=0$, the corresponding entanglement is always zero, indicating that there is no entanglement between the two qubits. Certainly this should be the case since there is no interaction between the two qubits. When U becomes nonzero, the entanglement exhibits many kinds of complex oscillations. For the cases of the moderately strong Coulomb interactions ($U=5$, 10, and 20) the entanglement shows seemingly irregular evolution as the time goes on. However, with further increasing U, the evolution of the entanglement becomes much more regular and exhibits the periodical oscillation. This demonstrates that entanglement is strongly influenced by the interaction between the two qubits. Let us consider the details of the entanglement for $U=40$ in Fig. 4(b). It is evident that the entanglement shows the small-amplitude oscillations. To understand what causes this kind of oscillation, the evolution of σ_{aa} is also plotted. It is clear that both the entanglement and σ_{aa} oscillate in phase.[24] Therefore, we believe this oscillation is mainly caused by the small-amplitude undulations in σ_{aa} and σ_{dd} and in σ_{bb} and σ_{cc} [see Fig. 4(c)]. Furthermore, the large-amplitude oscillation is examined also, as shown in Fig. 4(c). It can be seen that when the entanglement takes the largest value of 1 the probabilities of σ_{bb} and σ_{cc} are equal to 0.5. At this moment the two qubits are right in

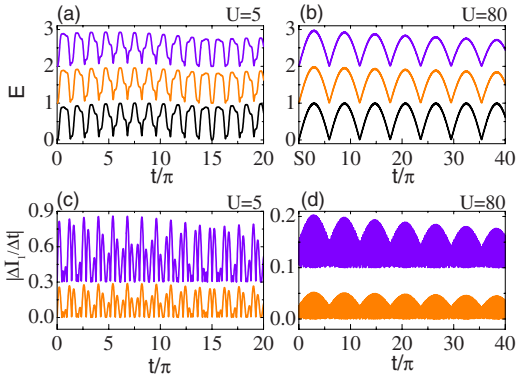

FIG. 5. (Color online) Time-dependent entanglement E with (a) $U=5$ and (b) $U=80$ for the different dephasing rates $D=0$, 1, and 2 which are shifted upward by 0, 1, and 2, respectively, from bottom to up. The corresponding time-dependent variation rates of the currents $|\Delta I_1/\Delta t|$ are shown in (c) $U=5$ and (d) $U=80$ for $D=1$ and 2. The curves with $D=2$ are shifted upward by (c) 0.3 and (d) 0.1.

the maximally entangled Bell state. In addition, it can also be seen that at a certain time the entanglement takes the value of 0. This indicates that there is no entanglement between the two qubits. By inspecting these positions with $E=0$, it can be found that only one diagonal element (σ_{bb} or σ_{cc}) equals the value of 1. This indicates that the system is in a pure state. Similar phenomena can be found in the large U limit [see Fig. 4(d)]. However, the small-amplitude oscillations in the entanglement curves disappear. At the same time, the small-amplitude oscillations in the curves of σ_{ii} $(i=a,b,c,d)$ also will vanish. This is exactly the reason why the entanglement curve becomes smooth.

B. Entanglement measurement

In this section we explore the scheme of extracting the quantum entanglement by means of the currents flowing through the two nearby QPC detectors. For convenience, weak measurement condition $D'=0.9D$ is still retained to minimize the effect of the decoherence in both the weak $(U=5)$ and strong $(U=80)$ Coulomb interaction cases. First, the corresponding time-dependent evolutions of the entanglement are plotted in Figs. 5(a) and 5(b), respectively. We can see that the entanglement in the case of $D\neq 0$ will evolve with the same period as that of $D=0$, indicating that the oscillation period of the entanglement is independent of the measurement process. However, the oscillation amplitude decays when the time t becomes large and, moreover, will decay more quickly for a larger D. This demonstrates that the measurement process will induce the decay of the entanglement. Second, we plot the time-dependent variation rate of the corresponding current $|\Delta I_1/\Delta t|$ for $D\neq 0$ [see Figs. 5(c) and 5(d)]. Let us pay attention to the strong $U=80$ case [see Figs. 5(b) and 5(d)]. We can see that the current variation rate shows the high-frequency oscillation with a long-period modulation oscillation. Very surprisingly, this long-period modulation of $|\Delta I_1/\Delta t|$ shows a perfect in-phase evolution with the corresponding entanglement. They approach the maximum or minimum position simultaneously. This indicates that we can obtain the maximal or minimal entanglement information easily from the $|\Delta I_1/\Delta t|$ curves. By a further comparison one can find that the extra evolution details of the entanglement information and the measured-induced dephasing can also be obtained from $|\Delta I_1/\Delta t|$. Therefore, the entanglement of the two strongly coupled qubits can be extracted based simply on the local measurement. As a consequence we have found an effective method to measure the two-qubit entanglement information.

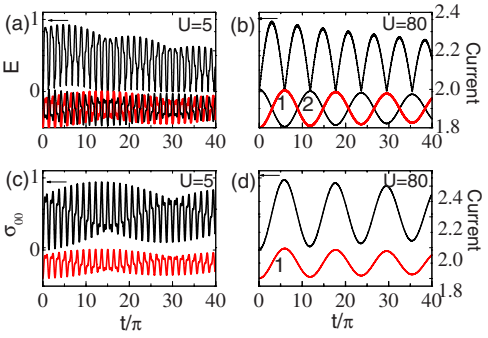

FIG. 6. (Color online) The time-dependent entanglement E and the corresponding currents $I_1(t)$ (label 1) and $I_2(t)$ (label 2) in the cases of (a) $U=5$ and (b) $U=80$. The time-dependent probabilities σ_{00} and the corresponding current $I_1(t)$ in the cases of (c) $U=5$ and (d) $U=80$. The parameters used for calculations are chosen to be $D=2$.

In the weak Coulomb interaction case of $U=5$, however, this kind of correspondence between the entanglement and $|\Delta I_1/\Delta t|$ can no longer be found and only limited information about the entanglement can be extracted. This indicates that this measurement method is not quite valid in the weakly coupled two-qubit system. One may wonder why it works well only in the strongly coupled two-qubit case. As a matter of fact its physical picture is particularly intuitive. When the Coulomb interaction is strong enough, the two-qubit electrons merely occupy states $|01\rangle$ and $|10\rangle$ with probability occupying state $|00\rangle$ or $|11\rangle$ being zero, which is reduced to the measurement of the single qubit. Hence, if the interaction is strong enough, the entanglement can be measured by a local measurement.

Can the two-qubit entanglement be directly extracted from the QPC currents? In Fig. 6 further investigation is conducted to discover the relationship between the currents $I_{1,2}(t)$ and the two-qubit entanglement. First, the weak interaction $U=5$ case is considered in Fig. 6(a). By comparing the entanglement and the corresponding currents, one can find that although both of them show the seemingly irregular evolution as the time goes on, the minimal entanglement positions are exactly at the places where the peaks or the troughs of the currents appear. This correspondence relation between the currents and the entanglement is still correct even at $U=80$ as clearly shown in Fig. 6(b). However, it is also difficult to extract more information directly from the currents. Therefore, we can only extract *partial* information of the two-qubit entanglement according to the detector currents in both the weak and strong U cases. One may wonder what on earth the detector currents reflect. Therefore, we plot the curves of the current $I_1(t)$ and the probability $\sigma_0=\sigma_{aa}+\sigma_{bb}$

which denotes the electron occupying QD0 in qubit 1 in Figs. 6(c) and 6(d), respectively. It is clear that no matter how strong the Coulomb interaction U is, the current $I_1(t)$ always oscillates in the same way as σ_{00} does. This verifies that the detector current I_1, in nature, completely reflects the electron-occupation probability in QD0 of qubit 1. In addition, it should be emphasized that, as estimated in Ref. 21, the oscillation amplitude of the current may be tuned in pA range and can be measured experimentally.

V. CONCLUSION

In conclusion, quantum measurement of the entanglement between two quantum-dot qubits has been investigated using the modified rate equations. It is found that the measurement process will induce the decaying of the quantum entanglement and the electron-occupation probabilities. Especially, our results indicate that when the two qubits are coupled by the sufficiently strong interactions, the entanglement between two qubits can be fully extracted by the local measurement via the current flowing through the QPC detectors.

ACKNOWLEDGMENTS

This work is financially supported by the NSFC under Grants No. 10811140163 and No. 10604005 and the Excellent Young Scholars Research Fund of Beijing Institute of Technology (Grant No. 2006Y0713). Z.T.J. wishes to thank Jun-Gang Li and Jie Yang for valuable discussions.

*jiangzhaotan@hotmail.com

[1] D. Bouwmeester, A. Ekert, and A. Zeilinger, *The Physics of Quantum Information* (Springer, Berlin, 2000).
[2] T. Tanamoto, Phys. Rev. A **64**, 062306 (2001); **61**, 022305 (2000).
[3] A. N. Korotkov, Phys. Rev. A **65**, 052304 (2002).
[4] R. Ruskov and A. N. Korotkov, Phys. Rev. B **67**, 241305(R) (2003).
[5] A. N. Jordan, B. Trauzettel, and G. Burkard, Phys. Rev. B **76**, 155324 (2007).
[6] R. Ruskov, A. N. Korotkov, and A. Mizel, Phys. Rev. B **73**, 085317 (2006).
[7] X. B. Wang, J. Q. You, and F. Nori, Phys. Rev. A **77**, 062339 (2008).
[8] A. Blais, J. Gambetta, A. Wallraff, D. I. Schuster, S. M. Girvin, M. H. Devoret, and R. J. Schoelkopf, Phys. Rev. A **75**, 032329 (2007).
[9] J. Li and G. Johansson, Phys. Rev. B **75**, 085312 (2007).
[10] W. J. Mao, D. V. Averin, F. Plastina, and R. Fazio, Phys. Rev. B **71**, 085320 (2005); W. J. Mao, D. V. Averin, R. Ruskov, and A. N. Korotkov, Phys. Rev. Lett. **93**, 056803 (2004).
[11] C. Hill and J. Ralph, Phys. Rev. A **77**, 014305 (2008).
[12] A. N. Jordan and M. Buttiker, Phys. Rev. Lett. **95**, 220401 (2005).
[13] T. Tanamoto and X. Hu, Phys. Rev. B **69**, 115301 (2004); J. Phys.: Condens. Matter **17**, 6895 (2005).
[14] M. Steffen, M. Ansmann, R. C. Bialczak, N. Katz, E. Lucero, R. McDermott, M. Neeley, E. M. Weig, A. N. Cleland, and J. M. Martinis, Science **313**, 1423 (2006).
[15] Y. Hasegawa, R. Loidl, G. Badurek, S. Filipp, J. Klepp, and H. Rauch, Phys. Rev. A **76**, 052108 (2007).
[16] A. G. Kofman, Q. Zhang, J. M. Martinis, and A. N. Korotkov, Phys. Rev. B **75**, 014524 (2007).
[17] T. Tanamoto and S. Fujita, Phys. Rev. B **72**, 085335 (2005).
[18] M. R. Sakr, H. W. Jiang, E. Yablonovitch, and E. T. Croke, Appl. Phys. Lett. **87**, 223104 (2005).
[19] S. A. Gurvitz and Ya. S. Prager, Phys. Rev. B **53**, 15932 (1996); S. A. Gurvitz, *ibid.* **56**, 15215 (1997).
[20] Here, we introduce $E_{ba}=E_{01}-E_{00}$, $E_{ca}=E_{10}-E_{00}$, $E_{da}=E_{11}-E_{00}$, $E_{cb}=E_{10}-E_{01}$, $E_{db}=E_{11}-E_{01}$, and $E_{dc}=E_{11}-E_{10}$; and $U_{ba}=U_{00,11}-U_{00,10}$, $U_{ca}=U_{01,10}-U_{00,10}$, $U_{da}=U_{01,11}-U_{00,10}$, $U_{cb}=U_{01,10}-U_{00,11}$, $U_{db}=U_{01,11}-U_{00,11}$, and $U_{dc}=U_{01,11}-U_{01,10}$.
[21] S. A. Gurvitz, Phys. Rev. Lett. **85**, 812 (2000); Z. T. Jiang, J. Peng, J. Q. You, and H. Z. Zheng, Phys. Rev. B **65**, 153308 (2002); Z. T. Jiang, J. Q. You, and H. Z. Zheng, J. Appl. Phys. **94**, 2142 (2003); Z. T. Jiang, J. Yang, and Q. Z. Han, J. Phys.: Condens. Matter **20**, 075210 (2008).
[22] M. Horodecki, P. Horodecki, and R. Horodecki, Phys. Lett. A **223**, 1 (1996).
[23] A. Peres, Phys. Rev. Lett. **77**, 1413 (1996).
[24] As we know, all four Bell states $\frac{1}{\sqrt{2}}(|00\rangle \pm |11\rangle)=\frac{1}{\sqrt{2}}(|a\rangle \pm |d\rangle)$ and $\frac{1}{\sqrt{2}}(|01\rangle \pm |10\rangle)=\frac{1}{\sqrt{2}}(|b\rangle \pm |c\rangle)$ are the maximally entangled states and the entanglement is closely related to these four Bell states. Whenever the system evolves into any Bell state, an entanglement peak will be observed, which induces the entanglement and the σ_{aa} oscillate in phase. When U is large enough, the two electrons will be inclined to occupy two diagonal QDs with larger probabilities than those in two nearest QDs. Therefore the probabilities of $\sigma_{aa,dd}$ become zero in the case of $U\rightarrow\infty$. Thus the entanglement related to states $|00\rangle$ and $|11\rangle$ diminishes and only that between $|01\rangle$ and $|10\rangle$ survives. So the small-amplitude oscillations disappear for large U.